




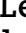



De novo DHDDS variants cause a neurodevelopmental and neurodegenerative disorder with myoclonus

Serena Galosi,¹ Ban H. Edani,^{2,3}  Simone Martinelli,⁴ Hana Hansikova,⁵ Erik A. Eklund,⁶ Caterina Caputi,¹ Laura Masuelli,⁷ Nicole Corsten-Janssen,⁸ Myriam Srour,^{9,10} Renske Oegema,¹¹ Daniëlle G. M. Bosch,¹¹ Colin A. Ellis,¹² Louise Amlie-Wolf,¹³ Andrea Accogli,^{9,10} Isis Atallah,¹⁴ Luisa Averdunk,¹⁵ Kristin W. Barañano,¹⁶ Roberto Bei,¹⁷ Irene Bagnasco,¹⁸  Alfredo Brusco,¹⁹ Scott Demarest,^{20,21} Anne-Sophie Alaix,²² Carlo Di Bonaventura,¹  Felix Distelmaier,¹⁵ Frances Elmslie,²³  Ziv Gan-Or,^{10,24,25} Jean-Marc Good,¹⁴ Karen Gripp,¹³ Erik-Jan Kamsteeg,²⁶ Ellen Macnamara,²⁷ Carlo Marcelis,²⁸ Noëlle Mercier,²⁹ Joseph Peeden,³⁰ Simone Pizzi,³¹ Luca Pannone,³¹ Marwan Shinawi,³² Camilo Toro,²⁷ Nienke E. Verbeek,¹¹ Sunita Venkateswaran,³³ Patricia G. Wheeler,³⁴ Lucie Zdrzilova,⁵ Rong Zhang,^{2,3} Giovanna Zorzi,³⁵ Renzo Guerrini,³⁶ William C. Sessa,^{2,3}  Dirk J. Lefeber,³⁷  Marco Tartaglia,³¹ Fadi F. Hamdan,³⁸ Kariona A. Grabińska^{2,3,†} and  Vincenzo Leuzzi^{1,†}

[†]These authors contributed equally to this work.

Subcellular membrane systems are highly enriched in dolichol, whose role in organelle homeostasis and endosomal-lysosomal pathway remains largely unclear besides being involved in protein glycosylation. *DHDDS* encodes for the catalytic subunit (DHDDS) of the enzyme *cis*-prenyltransferase (*cis*-PTase), involved in dolichol biosynthesis and dolichol-dependent protein glycosylation in the endoplasmic reticulum. An autosomal recessive form of retinitis pigmentosa (retinitis pigmentosa 59) has been associated with a recurrent *DHDDS* variant. Moreover, two recurring *de novo* substitutions were detected in a few cases presenting with neurodevelopmental disorder, epilepsy and movement disorder.

We evaluated a large cohort of patients ($n = 25$) with *de novo* pathogenic variants in *DHDDS* and provided the first systematic description of the clinical features and long-term outcome of this new neurodevelopmental and neurodegenerative disorder. The functional impact of the identified variants was explored by yeast complementation system and enzymatic assay.

Patients presented during infancy or childhood with a variable association of neurodevelopmental disorder, generalized epilepsy, action myoclonus/cortical tremor and ataxia. Later in the disease course, they experienced a slow neurological decline with the emergence of hyperkinetic and/or hypokinetic movement disorder, cognitive deterioration and psychiatric disturbances. Storage of lipidic material and altered lysosomes were detected in myelinated fibres and fibroblasts, suggesting a dysfunction of the lysosomal enzymatic scavenger machinery. Serum glycoprotein hypoglycosylation was not detected and, in contrast to retinitis pigmentosa and other congenital

disorders of glycosylation involving dolichol metabolism, the urinary dolichol D18/D19 ratio was normal. Mapping the disease-causing variants into the protein structure revealed that most of them clustered around the active site of the DHDDS subunit. Functional studies using yeast complementation assay and *in vitro* activity measurements confirmed that these changes affected the catalytic activity of the cis-PTase and showed growth defect in yeast complementation system as compared with the wild-type enzyme and retinitis pigmentosa-associated protein. In conclusion, we characterized a distinctive neurodegenerative disorder due to *de novo* DHDDS variants, which clinically belongs to the spectrum of genetic progressive encephalopathies with myoclonus. Clinical and biochemical data from this cohort depicted a condition at the intersection of congenital disorders of glycosylation and inherited storage diseases with several features akin to of progressive myoclonus epilepsy such as neuronal ceroid lipofuscinosis and other lysosomal disorders.

- 1 Department of Human Neuroscience, Sapienza University, Rome 00185, Italy
- 2 Vascular Biology and Therapeutics Program, Yale University School of Medicine, New Haven, CT 06520, USA
- 3 Department of Pharmacology, Yale University School of Medicine, New Haven, CT 06520, USA
- 4 Department of Oncology and Molecular Medicine, Istituto Superiore di Sanità, Rome 00161, Italy
- 5 Department of Pediatrics and Inherited Metabolic Disorders, First Faculty of Medicine, Charles University in Prague and General University Hospital in Prague, Prague 12808, Czech Republic
- 6 Section for Pediatrics, Department of Clinical Sciences, Lund University, Lund 22184, Sweden
- 7 Department of Experimental Medicine, Sapienza University, Rome 00161, Italy
- 8 Department of Genetics, University of Groningen, University Medical Center Groningen, Groningen 9700, The Netherlands
- 9 Department of Pediatrics, McGill University, Montreal, QC H4A 3J1, Canada
- 10 Department of Neurology and Neurosurgery, McGill University, Montreal, QC H4A 3J1, Canada
- 11 Department of Genetics, University Medical Center Utrecht, Utrecht 3584 CX, The Netherlands
- 12 Department of Neurology, University of Pennsylvania, Philadelphia, PA 19104, USA
- 13 Division of Medical Genetics, Nemours/A I duPont Hospital for Children, Wilmington, DE 19803, USA
- 14 Division of Genetic Medicine, Lausanne University Hospital and University of Lausanne, Lausanne 1011, Switzerland
- 15 Department of General Pediatrics, Neonatology and Pediatric Cardiology, Medical Faculty and University Hospital Düsseldorf, Heinrich-Heine-University Düsseldorf 40225, Germany
- 16 Department of Neurology, Johns Hopkins School of Medicine, Baltimore, MD 21287, USA
- 17 Department of Clinical Sciences and Translational Medicine, University of Rome 'Tor Vergata', Rome 00133, Italy
- 18 Division of Neuropsychiatry, Epilepsy Center for Children, Martini Hospital, Turin 10128, Italy
- 19 Department of Medical Sciences, University of Torino & Medical Genetics Unit, Città della Salute e della Scienza University Hospital, Turin 10126, Italy
- 20 Children's Hospital Colorado, Aurora, CO 80045, USA
- 21 Department of Pediatrics, University of Colorado School of Medicine, Aurora, CO 80045, USA
- 22 Hôpital Universitaire Necker Enfants Malades APHP, Paris 75015, France
- 23 South West Thames Regional Genetics Service, St. George's Healthcare NHS Trust, London SW17 0QT, UK
- 24 Montréal Neurological Institute and Hospital, McGill University, Montreal, QC H3A 2B4, Canada
- 25 Department of Human Genetics, McGill University, Montréal, QC H3A 0C7, Canada
- 26 Department of Human Genetics, Radboud University Medical Centre, Nijmegen 6525, The Netherlands
- 27 Undiagnosed Diseases Program, National Institutes of Health, Bethesda, MD 20892-2152, USA
- 28 Department of Clinical Genetics, Radboud University Medical Centre, Nijmegen 6525, The Netherlands
- 29 Service d'Epileptologie et Médecine du handicap, Hôpital Neurologique, Institution de Lavigny, Lavigny 1175, Switzerland
- 30 East Tennessee Children's Hospital, University of Tennessee Department of Medicine, Knoxville, TN 37916, USA
- 31 Genetics and Rare Diseases Research Division, Ospedale Pediatrico Bambino Gesù, IRCCS, Rome 00146, Italy
- 32 Department of Pediatrics, Washington University School of Medicine, St. Louis, MO 63110, USA
- 33 Division of Neurology, Children's Hospital of Eastern Ontario, Ottawa ON K1H 8L1, Canada
- 34 Arnold Palmer Hospital for Children, Orlando, FL 32806, USA
- 35 Department of Pediatric Neurology, IRCCS Foundation Carlo Besta Neurological Institute, Milan 20133, Italy

- 36 AOU Meyer, Pediatric Neurology, Neurogenetics and Neurobiology Unit and Laboratories, Meyer Children's Hospital, University of Florence, Florence 50139, Italy
- 37 Department of Neurology, Translational Metabolic Laboratory, Donders Institute for Brain, Cognition and Behavior, Radboud University Medical Centre, Nijmegen 6525 AJ, The Netherlands
- 38 Division of Medical Genetics, Department of Pediatrics, CHU Sainte-Justine and University of Montreal, Montreal, QC H3T1C5, Canada

Correspondence to: Vincenzo Leuzzi
 Unit of Child Neurology and Psychiatry
 Department of Human Neuroscience Sapienza University of Rome
 Via dei Sabelli 108, 00185, Rome, Italy
 E-mail vincenzo.leuzzi@uniroma1.it

Keywords: myoclonus epilepsy; movement disorder; neurodegenerative disorder; congenital disorders of glycosylation; dolichol

Abbreviations: CDG = congenital disorder of glycosylation; cis-PTase = cis-prenyltransferase; Dol-P = dolichyl monophosphate; ER = endoplasmic reticulum; GDD = global developmental delay; ID = intellectual disability; NgBR = Nogo-B receptor

Introduction

DHDDS (MIM*608172) encodes for the dehydrodolichyl diphosphate synthase subunit DHDDS, which in a complex with NgBR (also termed Nogo-B receptor) encoded by the *NUS1* gene, constitutes the cis-prenyltransferase (cis-PTase), a branch point enzyme of the mevalonate pathway. Cis-PTase is located in the endoplasmic reticulum (ER) and is involved in the biosynthesis of dolichyl monophosphate (Dol-P), an essential lipid serving as a glycosyl moiety carrier for protein N-glycosylation and as a carrier of dolichol-linked monosaccharide donors (Dol-P-Glc and Dol-P-Man) for O-mannosylation, C-mannosylation and glycosylphosphatidylinositol (GPI) anchor formation.^{1,2} The structure of the eukaryotic enzyme as well as the mechanism through which DHDDS and NgBR stabilize each other, which is crucial for cis-PTase activity,^{3–5} has recently been clarified.^{2,6} Dolichols size varies between species and is determined by the given cis-PTase. In humans, DHDDS determines the number of isoprenoid units⁶ that are commonly between 17 and 20, with a preponderance of dolichol-19 (D19).⁷

Protein N-glycosylation is a post-translational modification crucial to protein folding, oligomerization and intracellular sorting and transport. Molecular defects in genes involved in N-glycan biosynthesis belong to a family of metabolic disorders, collectively known as congenital disorders of glycosylation (CDGs).^{8,9} These diseases share an abnormal pattern of protein or lipid glycosylation and major nervous system involvement in the context of multisystemic disease. CDG subtypes with autosomal recessive defects in dolichol biosynthesis (DHDDS-CDG, SRD5A3-CDG, *NUS1*-CDG and *DOLK*-CDG)^{10–12} have been reported, and most are detectable by routine CDG screening of serum transferrin via isoelectric focusing or mass spectrometry.

Defects in the dolichol oligosaccharide assembly pathway cause accumulation of underglycosylated misfolded glycoproteins driving a chronic induction of the unfolded protein response pathway and ER stress, along with apoptosis and regeneration.^{13,14} A marked induction of ER stress and impaired N-linked glycosylation has also been observed in *NUS1* mutant fibroblasts, in association with intralysosomal cholesterol storage as seen in Niemann Pick type C disease.⁴

Despite the crucial role of dolichol synthesis in protein glycosylation in several tissues, germline mutations in *DHDDS* have only recently been associated with a complex multisystem phenotype in an individual exhibiting intrauterine growth deficiency, micropenis, hepatomegaly, renal failure, axial hypotonia, increased appendicular tone, severe global developmental delay (GDD) and refractory epilepsy, who died at 8 months in status epilepticus. Analysis of skin fibroblasts revealed variable amounts of truncated dolichol and protein-linked N-glycans. This condition was associated with biallelic loss-of-function mutations and a CDG type I pattern of glycosylation.¹⁵

A recurrent homozygous variant in *DHDDS* (c.124A>G; p.Lys42Glu) was found in consanguineous families with non-syndromic retinitis pigmentosa (RP type 59).^{16–19} In these patients, D18 becomes the dominant species, with altered plasma and urinary D18/D19 ratios.²⁰

Two additional recurrent pathogenic variants, i.e. p.Arg37His and p.Arg211Gln, have been reported in seven individuals from unrelated families with intellectual disability (ID), epilepsy, tremor, myoclonus and movement disorder.^{21–23} The p.Arg37His variant falls in an evolutionary conserved stretch of five amino acid residues (position 34–38), which corresponds to the catalytic domain of the enzyme.^{2,21} Crystal structure and mutagenesis studies demonstrated that Arg211 is critical in homoallylic binding to the isopentenyl diphosphate (IPP) substrate.² Although generalized epilepsy, tremor and ID seem to be the main features associated with *de novo* *DHDDS* missense mutations, available clinical information is very limited and detailed genotype-phenotype correlation is lacking. A dominant-negative mechanism has been proposed to explain the allelic heterogeneity associated with *DHDDS*-related disorders.²³

Given the shared metabolic pathway, *de novo* variants in *NUS1* have recently been associated with a clinical phenotype that overlaps with that described for *de novo* *DHDDS* pathogenic variants, namely ID, well-controlled generalized epilepsy, prominent tremor/myoclonus, ataxia and parkinsonism with a slowly progressive course.^{21,24,25} *NUS1* variants were reported in isolated early-onset Parkinson's disease.²⁶ A homozygous *NUS1* variant was described in a patient with severe neurological impairment, refractory epilepsy and congenital disorder of glycosylation.⁴

In this study, we delineated the clinical phenotype associated with dominant DHDDS variants through the long-term clinical observation of a large cohort of patients. We provided the first genotype–phenotype correlation analysis through functional characterization of reported DHDDS variants using yeast complementation and enzymatic assays. We also confirmed the role of the NgBR/DHDDS complex dysfunction in early-onset neurodevelopmental and neurological disorders including myoclonus syndromes.

Materials and methods

Patients

We collected clinical and molecular data of 25 patients from 24 unrelated families with likely pathogenic/pathogenic variants in DHDDS from different clinical centres in Europe, USA and Canada through international clinical collaborations and networking (GeneMatcher).²⁷ Three patients (Patients 1–3) were previously reported with limited clinical data in Hamdan *et al.*²¹

For each confirmed case, the referring physician completed a case review and returned pseudo-anonymized data including developmental, neurological, behavioural and epilepsy medical history, metabolic studies, EEGs and neuroimaging data. Seizure types were classified using the International League Against Epilepsy (ILAE) criteria,²⁸ or in more descriptive terms when the seizure phenomenology did not fit this classification terminology. Patients were evaluated according to developmental and cognitive functioning scales routinely used in the participating centres. Written informed consent was locally obtained for all participants.

Molecular genetic investigations and in silico modelling

The DHDDS (NM_024887) pathogenic variants reported herein were all identified by clinical (19/25) or research (5/25) whole exome sequencing (WES), except for one which was identified by research whole genome sequencing (WGS) (Supplementary Table 1). With the exception of a single-residue deletion (Lys42) documented in a single patient, they were mostly missense. In 22 of the 23 tested families, direct Sanger sequencing confirmed the *de novo* origin of the DHDDS variant. In Family 4, segregation analysis documented mosaicism (p.Arg211Gln) in the father. Parental genomic DNA specimens were not available in Family 12 (p.Arg37His). In both cases, the identified variants were recurrent and demonstrated to occur as *de novo* events in multiple instances. The clinical relevance of the identified variants was assessed using the American College of Medical Genetics and Genomics (ACMG) guidelines for variant interpretation (Supplementary Table 1A).^{29,30}

Mapping of the *de novo* DHDDS mutations was achieved using the previously solved crystal structure of human NgBR/DHDDS enzyme in complex with Mg²⁺ and IPP substrate (PDB ID: 6W2L). PyMOL software was used to model the location and binding interactions of individual mutations.

Functional characterization of DHDDS missense variants

Detailed methods for expression and purification of the NgBR/DHDDS complex, cis-PTase activity assay and yeast complementation assay are available in the Supplementary material.

Metabolic studies

Detailed methods for glycosylation profiling through liquid chromatography combined with tandem mass spectrometry (LC-MS/MS) analysis of serum transferrin and dolichol content analysis in urine by LC-MS/MS are available in the Supplementary material.^{31–33}

Data availability

The authors confirm that the data supporting the findings of this study are available within the article and its Supplementary material.

Results

Clinical description

We studied 25 patients (17 males and eight females) aged 4 to 59 years. Eleven were young adults or adults (age range 18–59 years). Most patients were born from normal pregnancies and deliveries, with normal growth parameters and neonatal examinations. Detailed descriptions of neurodevelopmental, epileptic and motor features are reported in Table 1 and Supplementary Table 1. Extensive clinical reports for 14 of 25 patients are available in the Supplementary material.

Presenting features and disease evolution

Initial signs of neurodevelopmental and/or neurological impairment were noticed during infancy in 22 of 25 patients (age at symptom onset: range 1–24 months, median 12 months). Patients 17 and 23, now 44 and 16 years old, who manifested their initial clinical symptoms at age 5 and 3, respectively, had the latest disease onset and mildest phenotype.

GDD with or without hypotonia was the most frequent presenting symptom (23 of 25 patients). Additional features frequently reported at onset included tremor and seizures. Ataxia was an early symptom in 6 of 25 patients. In two patients, parents reported a neurological regression beginning from early disease stages.

The combination of GDD and tremor occurred in 11 of 25 patients, four of whom also experienced seizures, thus manifesting the core triad of the condition from onset.

Neurological deterioration was described in most patients (17 of 25), with no obvious genetic, demographic or clinical factor influencing prognosis. Seven patients (Patients 1, 6, 9, 10, 13, 19 and 21) exhibited prominent cognitive decline. Progression occurs over years or decades. In some patients, there were periods of rapid deterioration while in others progression was gradual. Stepwise neurological deterioration with multiple phases of regression was observed in Patients 1, 9 and 12. The outcomes of Patients 1 and 19, respectively 39 and 17 years, were particularly severe with intense fatigue, autonomic dysregulation (bladder, temperature, heart rate, breathing) and dementia with akinetic mutism.

Neurodevelopmental, cognitive and behavioural phenotype

All patients except one had ID, which was severe in 12, moderate in six and mild in five. Patient 8 had normal development up to 18 months of age, after which developmental issues were first noticed in relation to epilepsy onset. Patients were able to sit between 9 and 18 months, walk between 13 and 36 months,

Table 1 Clinical and genetic features of 25 patients with *de novo* DHDDS variants

Patient ^a	DHDDS variant	Presenting symptoms	Cognitive and psychiatric features	Epilepsy ^b	Movement disorder
1/M First mo/39 y	c.632G>A, p.(Arg211Gln)	Hypotonia, GDD, tremor, myoclonus	Severe ID, autistic traits, impulsivity, anxiety, cognitive decline, catatonia	5 y/Gen/absence/no	Tremor, ataxia, parkinsonism, dystonia
2/F 1 y/7.3 y	c.632G>A, p.(Arg211Gln)	GDD, tremor, myoclonus	Moderate ID	–	Tremor, myoclonus
3/M 1 y/6 y	c.110G>A, p.(Arg37His)	Hypotonia, GDD, tremor, epilepsy	Mild ID; hyperactivity	1 y/Gen/FS, My, MA, absence/no	Tremor, ataxia
4/F 10 mo/13 y	c.632G>A, p.(Arg211Gln)	GDD, epilepsy	Severe ID; autistic traits, anxiety	10 mo/Gen/GTC, absence/yes	Tremor, ataxia
5/M 6 mo/4.5 y	c.632G>A, p.(Arg211Gln)	Hypotonia, tremor, joint laxity	moderate ID; hyperactivity	–	Tremor, ataxia, spasticity
6/M 15 mo/26 y	c.632G>A, p.(Arg211Gln)	DD, tremor, ataxia	Severe ID, cognitive decline, psychosis	10 y/Gen/GTC/no	Tremor, myoclonus, parkinsonism, dystonia, spasticity
7/M 11 mo/19 y	c.109C>T, p.(Arg37Cys)	Epilepsy, GDD	Severe ID	11 mo/Gen/My, At, absence, GTC/yes	Tremor, myoclonus, chorea
8/F 1.5 y/31 y	c.109C>T, p.(Arg37Cys)	FS, GDD	Moderate ID, ADHD, anxiety, oppositional behaviour, autistic traits	2 y/Gen/GTC, Tn, absence/yes	Tremor, ataxia, myoclonus, dystonia
9/M 2 y/16 y	c.698C>G, p.(Pro233Arg)	DD, tremor, neurological regression	Mild ID, OCD	10 y/Gen/Tn/no	Chorea, myoclonus
10/M 7 mo/6.5 y	c.110G>A, p.(Arg37His)	GDD, neurological regression, FS	Severe ID, ASD	4 y/Gen/Absence, At/no	Stereotypies
11/F First mo/24 y	c.632G>A, p.(Arg211Gln)	GDD, epilepsy, myoclonus, ataxia	Severe ID, ADHD	11 mo/Gen/My/yes	Ataxia, myoclonus, tremor, dystonia, parkinsonism
12/M Infancy/59 y	c.110G>A, p.(Arg37His)	GDD	Mild ID, impulsivity, executive dysfunction	19 years/Gen/GTC/no	Ataxia, myoclonus, tremor, parkinsonism, spasticity
13/F 2 y/34 y	c.109C>T, p.(Arg37Cys)	DD, myoclonus, ataxia, stereotypies	Severe ID, anxiety, phobias, catatonia	Childhood/Gen/GTC/no	Myoclonus, ataxia, stereotypies
14/F 2 y/34 y	c.109C>T, p.(Arg37Cys)	DD, myoclonus, ataxia, stereotypies	Severe ID, anxiety, phobias	Childhood/Gen/GTC/no	Myoclonus, ataxia, stereotypies
15/M First mo/16 y	c.104G>A, p.(Gly35Glu)	craniosynostosis, GDD	Moderate ID	3 y/Fc/partial/no	Tremor, chorea, myoclonus, dystonia, ataxia
16/F NR/4 y	c.632G>A (p.Arg211Gln)	GDD, epilepsy	GDD	21 mo/Gen/My, At, absence/no	–
17/M 5 y/44 y	c.632G>A (p.Arg211Gln)	FS	Psychosis	5 y/Gen/absence, My, GTC/no	Myoclonus, tremor, ataxia
18/M 1 y/17 y	c.638G>A, p.(Ser213Asn)	DD, tremor, epilepsy	Severe ID	1 y/Gen/absence, MA, Tn, GTC/yes	Tremor, ataxia, myoclonus, parkinsonism
19/F 6 mo/18 y	c.614G>A, p.(Arg205Gln)	DD, epilepsy, tremor, myoclonus, ataxia	Mild ID, ADHD, anxiety, oppositional behaviour	1 y/Gen/absence/no	Tremor, ataxia, dystonia, parkinsonism
20/M 1 y/14 y	c.632G>A (p.Arg211Gln)	GDD, epilepsy	Moderate ID, Anxiety, autistic traits	6 mo/Gen/absence, MA, GTC, Tn, At/yes	Tremor, ataxia, myoclonus, dystonia, parkinsonism
21/M 18 mo/16 y	c.104G>A, p.(Gly35Glu)	GDD, hypotonia	Moderate ID, ASD	11 mo/Gen/GTC, absence, My, At/yes	Ataxia, tremor, chorea, rigidity
22/M 6 mo/14 y	c.632G>A, p.(Arg211Gln)	GDD, hypotonia	Severe ID	2 y/Gen/GTC, absence/no	Ataxia, myoclonus, tremor
23/F 3 mo/16 y	c.632G>A, p.(Arg211Gln)	GDD, tremor, clumsiness	Mild ID	–	Tremor
24/F 7 mo/22 y	c.124_126del, p.(Lys42del)	GDD, epilepsy	Severe ID, ASD	7 mo/Gen/FS, GTC, My, absence, At/yes	Tremor, myoclonus, parkinsonism
25/M 18 mo/7 y	c.110G>A, p.(Arg37His)	GDD, epilepsy	Moderate ID, hyperactivity	8 mo/Gen/FS, My, MA, absence/yes	Ataxia

Detailed clinical information is provided in [Supplementary Table 2](#) and [Supplementary material](#) as case reports. ADHD = attention-deficit/hyperactivity disorder; ASD = autism spectrum disorder; At = atonic; F = female; Fc = focal; FS = febrile seizures; Gen = generalized; GTC = generalized tonic-clonic; M = male; MA = myoclonic-atonic; Mo = months; My = myoclonic; NA = not assessed; OCD = obsessive compulsive disorder; Tn = tonic; y = year/years.

^aPatient number/sex/age of onset/age at follow-up.

^bEpilepsy age of onset/epilepsy type/seizure type/resistance to anti-epileptic drugs (yes/no).

pronounce their first words after 3 years and, in those with milder cognitive impairment, speak in sentences after 4–5 years of age.

Patient 17 graduated from high school and attended community college, achieving above-average grades. Gross motor functioning was normal and he was an excellent swimmer and skier. He exhibited absence seizures since age of 5 years, myoclonus at 16 years and rare generalized tonic-clonic seizures (GTCS) in adulthood. Patient 12 complained of tremor from the age of 10 years and had his first epileptic seizures at the age of 19 years. He showed borderline intellectual functioning, though it was compatible with a normal employment in adulthood.

Relevant behavioural and/or neuropsychiatric comorbidities were reported in most patients (18 of 25) (Fig. 1, Table 1 and Supplementary material). Four patients presented a severe psychiatric outcome with psychosis and/or catatonia in advanced disease stage (adolescence to adulthood) (Patients 1, 6, 13 and 17).

Epilepsy

Epilepsy, reported in 22 of 25 patients, was a core feature of the disorder. Age at seizure onset ranged from 6 months to 10 years. Thirteen of 25 patients had infantile onset epilepsy (birth–2 years), 8 of 25 had childhood onset epilepsy (3–12 years), and one patient (Patient 12) had GTCS onset at 19 years. Febrile seizures (myoclonic, absence or GTCS) were reported in 7 of 25 and were part of the presenting features (11–25 months of age) in 6 of 25 patients (Patients 3, 7, 8, 10, 17, 24 and 25), preceding afebrile seizure onset. In Patient 7, seizures started after vaccination. Photosensitivity was observed in five patients (Patients 1, 18, 19, 24 and 25).

Generalized epilepsy including myoclonic-atic tonic epilepsy was reported in 21 of 25 patients with absence (15 of 25), GTC (13 of 25),

myoclonic (8 of 25) and atonic (6 of 25) being the most frequent seizure types. The distribution of seizure types is summarized in Table 1 and Fig. 1. Absence seizures included typical absences, atypical absences, myoclonic absences and absences with eyelid myoclonia (Supplementary Table 1). Patients 9, 18 and 20 had frequent nocturnal seizures, which were tonic in Patients 9 and 20, whereas Patient 18 had GTCS seizures. Twenty of 25 patients presented multiple seizure types, typically two to four.

Epilepsy was well controlled with anti-epileptic drugs (AEDs) in 13 of 25 patients, while nine patients had drug-resistant seizures. All patients with childhood onset epilepsy (Patients 1, 6, 9, 10 and 13–17) were well controlled under AED therapy. Among patients with infantile onset epilepsy, 9 of 13 had drug-resistant epilepsy non-responsive to combinations of several conventional AEDs, and 4 of 13 were well controlled using valproate alone, or in combination with levetiracetam or clobazam.

Generalized EEG abnormalities were reported in 16 of 22 epileptic patients. EEG recordings in 12 of 22 patients showed bursts of ictal and interictal generalized slow spike and wave complexes (2–4 Hz), sometimes predominantly on the frontal region, in association with generalized slow activity and/or diffuse slowing of the posterior dominant rhythm or abnormal background activity. Ictal slow spike-wave complexes correlated with absences, eyelid myoclonia, myoclonic seizures and atonic events (head drops, falls) (Patients 1, 3, 4, 7, 8, 10, 18, 19, 21, 22 and 25) (Fig. 2).

Epilepsy usually improved or resolved from adolescence and epileptiform abnormalities disappeared over the disease course (Supplementary material). The most effective AEDs, alone or in combination were valproate (11 of 22), levetiracetam (8 of 22), clobazam (6 of 22) and clobazam (6 of 22); other drugs were less

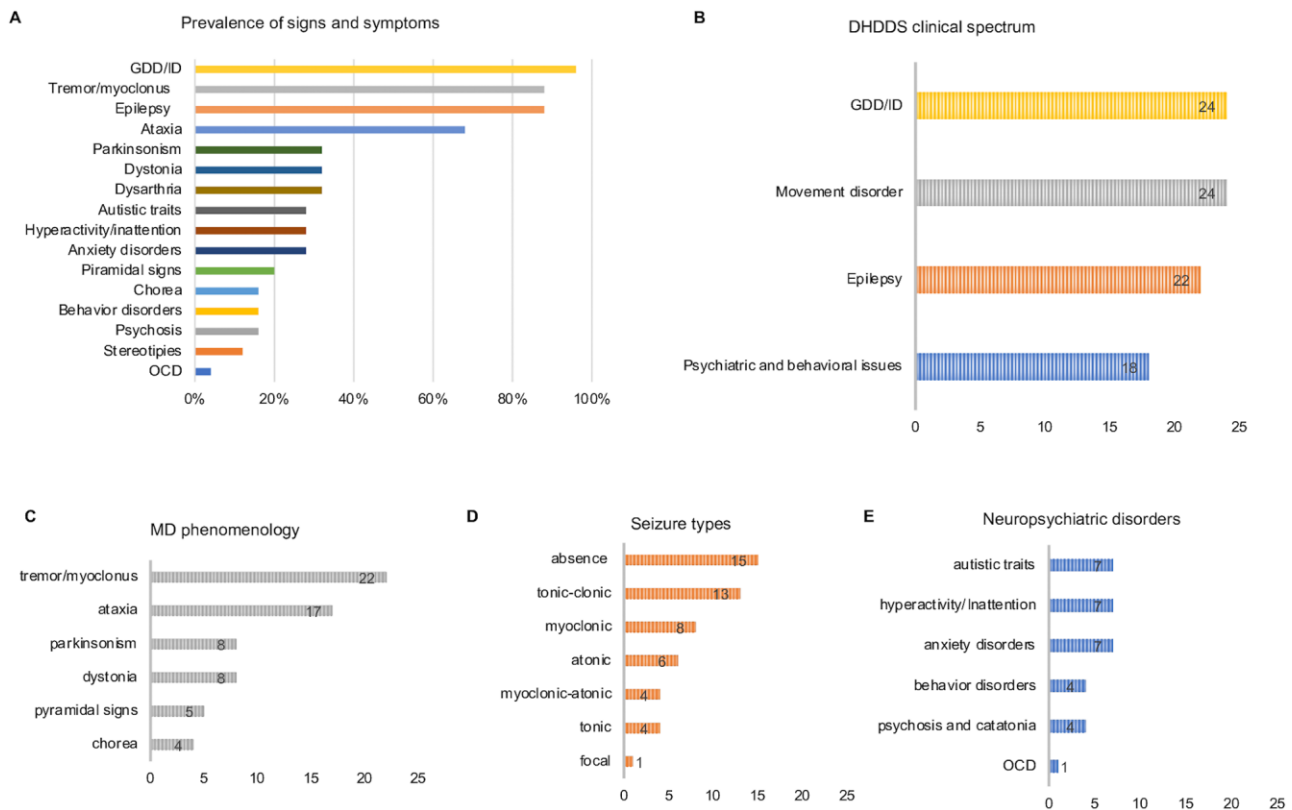


Figure 1 Phenotypic spectrum associated with *de novo* DHDDS variants. (A) Prevalence of signs and symptoms in patients with *de novo* DHDDS variants ($n = 25$). (B) Frequency of the core clinical features in patients with *de novo* DHDDS variants. (C) Frequency of movement disorder (MD) subtypes; 20 of 25 patients had >1 movement disorder subtype. (D) Frequency of seizure types. (E) Frequency of neuropsychiatric features. The number of affected patients is reported in each graph bar (B–E).

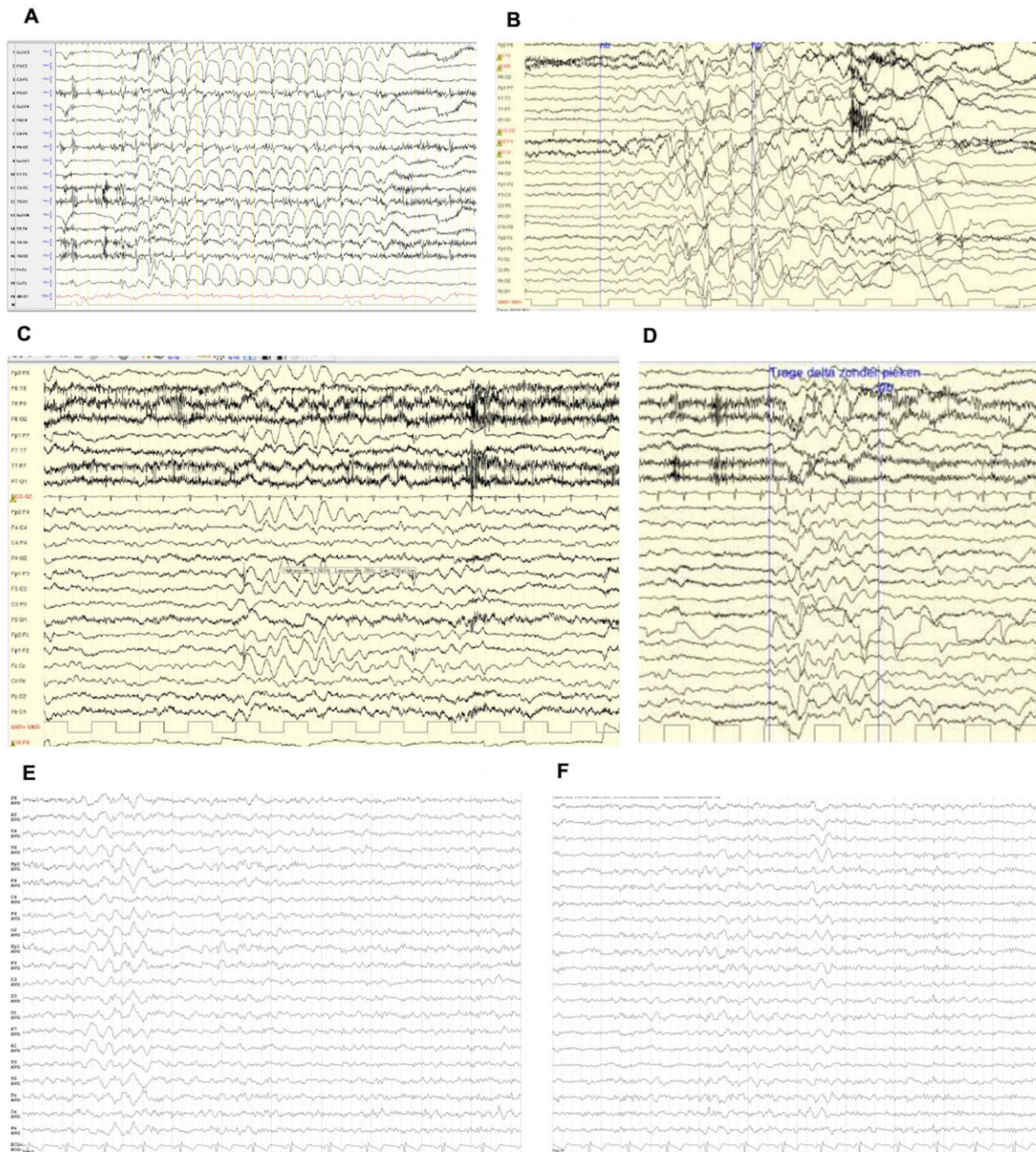


Figure 2 Examples of EEG recordings in patients with *de novo* DHDSD variants. (A) Patient 20, awake EEG at the age of 12 years showing generalized 3 Hz spike-wave discharges during an absence seizure. (B) Patient 16, awake EEG at the age of 4 years showing generalized 2 Hz irregular spike and wave activity followed by high amplitude slow waves and by an electrodecremental event. Clinically, during the spike-wave complexes, the patient lies with eyes open and manifests an axial myoclonic jerk. (C) Awake EEG of Patient 16 at the age of 4 years showing sequences of interictal frontal delta waves (2.5 Hz) lasting several seconds. (D) Same patient as in C: polymorphic interictal diffuse delta and theta activity. (E and F) Patient 12, interictal awake EEG at the age of 58 years showing a diffuse slowing and bursts of generalized rhythmic delta activity (GRDA).

effective, including lamotrigine (2 of 22), zonisamide (3 of 22), topiramate (2 of 22), ethosuximide (1 of 22), phenobarbital (1 of 22), primidone (1 of 22), lacosamide (1 of 22) and brivaracetam (1 of 22). Levetiracetam led to seizures worsening in Patient 8.

Movement disorder

Movement disorder, generally as bilateral distal intention and postural tremor/myoclonus of the upper limbs (Patients 1–5, 8, 15, 18, 19 and 23), was part of the clinical presentation in most of patients

(14 of 25), detected in the first months of life in some patients (Patients 3, 5, 8, 15 and 18) and sometimes associated with ataxia (Patients 1–5, 18, 19 and 21) and/or hypotonia (6 of 25). Patients 1, 2 and 23 underwent neurophysiological studies with back-averaged EEG that demonstrated a cortical origin of tremor.

Tremor tended to change over time in terms of distribution and type with involvement of the trunk and lower extremities and onset of rest tremor superimposed to the already present action and postural components (Patients 1, 6, 8, 12, 15, 19 and 21) (Supplementary Videos 1–5, available from figshare <https://doi.org/>

10.6084/m9.figshare.15106032.v1). Tremor became continuous over time, exacerbated by sudden lights, loud noises, stress, and movement (Patients 1, 8, 12 and 16; Supplementary Videos 1, 2 and 5). Facial involvement, particularly of the eyebrows and mouth, was observed in 8 of 25 patients (Patients 1, 6–8 and 11–14) (Supplementary Videos 1–5). Periodic exacerbations of tremor/myoclonus lasting hours to days (Patients 1 and 2) (Supplementary Video 1) and episodic weakness requiring hospitalization (Patients 1 and 9) were reported.

At follow-up, 24 of 25 patients had a movement disorder. In most of them (14 of 25), a complex pattern of movement disorder emerged over time (Patients 1, 6–9, 11, 12, 15, 18–21, 24 and 25) including ataxic features (Patients 2–5, 8, 12–16, 18–23 and 25), dystonic posturing of the upper and/or lower limbs (Patients 1, 6, 8, 11, 15 and 18–20) (Supplementary Video 2), parkinsonism (Patients 1, 6, 11, 12, 18–20 and 24) and chorea (Patients 7, 9, 16 and 22) (Fig. 1 and Table 1). Fluctuations in tremor and other MDs severity were observed in Patients 1, 8, 11, 18, 19 and 22. Parkinsonism with rigidity, rest tremor, bradykinesia and hypomimia was a late disease feature, which developed gradually from adolescence (Supplementary Videos 1 and 2). Over the disease course 8 of 25 patients developed speech abnormalities such as hypophonic and slow speech (Patients 1, 20 and 23), dysarthria (Patients 3, 8, 11, 12 and 19) and loss of speech/anarthria (Patients 1 and 6). Pyramidal signs were reported in 5 of 24 patients (Patients 5, 6, 12, 19 and 21).

Most patients did not receive treatment for movement disorder (21 of 25) and epilepsy treatment had a relatively mild effect on tremor and movement disorders. Piracetam was ineffective for cortical tremor in Patient 1, while a partial response was observed with high doses of clonazepam (up to 9 mg/day). Parkinsonism did not respond to levodopa, which instead increased impulsivity and hyperactivity. Interestingly, very low doses of risperidone (0.5 mg/day) or tetrabenazine (6.25 mg/day) were able to control the

severity of myoclonic episodes in advanced disease stage, while higher dosages induced akinetic status. In Patient 17 tremor responded to propranolol, while in Patient 24 a mild effect of benzodiazepines on cortical tremor was observed.

Associated features

Dysmorphisms were reported in a subgroup of patients (Fig. 3). The most recurrent features were altered dental architecture with wide spaced or missing teeth (Patients 2, 4 and 7) and generalized hypertrichosis with dark hair and thick eyebrows (Patients 1, 6, 9 and 15). Patient 15 developed axillary and pubic hair at age 4. Other dysmorphic features were wide-set almond-shaped eyes (Patients 7 and 9), upslanted palpebral fissures (Patients 4 and 7), flat/concave nasal bridge (Patients 4 and 7), prominent supraorbital ridge (Patients 7, 9 and 12), high frontal hairline (Patient 7), large mouth with full lips (Patient 7), high palate (Patient 2), bifid uvula (Patient 9), thick ear lobes (Patient 7), foetal pads (Patient 7) and first toe clinodactyly (Patient 4). Sagittal craniosynostosis was surgically repaired at 3 months of age in Patient 15. Hyperpigmentation at the right side of the thorax was seen in Patient 2.

Gastrointestinal issues with periods of severe constipation were reported in Patients 1 and 4, while recurrent abdominal pain and vomiting were reported in Patient 20. At the age of 14, Patient 9 was diagnosed with Crohn's disease and successfully treated with infliximab. Patient 17 underwent resection of a dysplastic rectal polyp at the age of 42 years with negative genetic testing for hereditary cancer predisposition. Patient 1 had fatty liver disease with hypercholesterolaemia, increased levels of gamma-glutamyl transferase and milder increase of serum transaminase.

Conjunctival telangiectasias was observed in Patients 1 and 20. Patient 20 was affected by a complex autoinflammatory disorder characterized by recurrent arthralgia of the knees, episcleritis,



Figure 3 Dysmorphic features. (A) Patient 7 facial dysmorphisms including wide-set almond-shaped eyes, upslanted palpebral fissures, high frontal hairline, prominent supraorbital ridge, concave nasal, large mouth with full lips, thick ear lobes, wide spaced teeth and foetal pads. (B) Patient 12 facial dysmorphisms including prominent supraorbital ridge and macrotia.

intermittent fever and suffered from an acute episode of purpura with erythrocyturia/haematuria and increased CRP and IgA, which significantly improved after steroid treatment. Skin biopsy was diagnostic for small vessel vasculitis demonstrating perivascular leucocyte infiltrates.

Brain imaging

Brain MRI, available for 24 of 25 patients, were normal in 23 of 24, with six patients (Patients 1, 2, 9, 15, 17 and 21) scanned more than once at different disease stages. Patient 1 had normal brain imaging up to the age of 27. At the age of 37, he started to severely deteriorate. Brain MRI showed T₂/FLAIR subcortical hyperintense non-enhancing foci localized to the frontal, temporo-occipital and visual cortices bilaterally with prominent involvement of calcarine cortex (Fig. 4A). A follow-up study at 10 months demonstrated severe and diffuse cortical and subcortical atrophy (Fig. 4B) including previously hyperintense areas, the dorsal striatum with prominent caudate involvement and cerebellum. ¹H-MRS demonstrated decreased N-acetylaspartate (NAA) peak and NAA/choline (Cho) ratio at the level of the caudate lesions, thus confirming neuronal degeneration. ¹H-MRS was performed and resulted normal in 4 of 24 patients. Stable corpus callosum thickening was documented in Patient 21. MRI of the spinal cord of Patient 17 showed a T5–T11 syrinx, which was stable on serial imaging from ages 35 to 43 years.

Metabolic features

CDG screening was performed by isoelectric focusing of plasma transferrin and resulted normal in 12 of 25 patients. Mass spectrometry analysis of plasma transferrin was subsequently performed in 5 of 25 patients, two of which showing marginally

abnormal glycosylation (Table 1). Urinary dolichol isoforms (D18/D19 ratio) were evaluated and resulted normal as compared with age-matched controls in 5 of 25 patients. Hypercholesterolaemia without hypertriglyceridaemia was reported in 3 of 25 patients.

Ultrastructural analysis of the skin biopsy from Patient 1 showed osmiophilic material deposits in myelinated fibres. Numerous single membrane-surrounded vacuoles containing lamellated membrane structures resembling phospholipids or other lipid-like material were observed in the axons of myelinated fibres (Fig. 5A–D). Cholesterol-like deposits associated with glycogen were evident in the cytoplasm of Schwann cells. In a small percentage of stroma fibroblasts large secondary lysosomes filled with different electron-density substances were found in the cytoplasm (Fig. 5E and F). Axillary skin biopsy revealed periodic acid-Schiff-positive bodies in eccrine glands in Patient 6.

Genetic findings and genotype–phenotype correlation

Fifteen individuals carried two previously reported DHDDS pathogenic variants (p.Arg37His and p.Arg211Gln),²¹ while 10 harboured new pathogenic/probable pathogenic variants (p.Gly35Glu, p.Arg37Cys, p.Lys42del, p.Arg205Gln, p.Ser213Asn and p.Pro233Arg) (Supplementary Tables 1 and 1A). Twenty-three variants were validated as *de novo* events, while parental mosaicism was demonstrated in Family 4, in which the asymptomatic father was found to be mosaic.

The most recurrent variant was p.Arg211Gln, which was detected in 11 of 25 patients (Patients 1 and 2 were previously reported with limited clinical information by Hamdan et al.²¹). Four of 25 patients had the previously reported p.Arg37His change^{21,22} (Patient 3 was previously reported previously with limited clinical

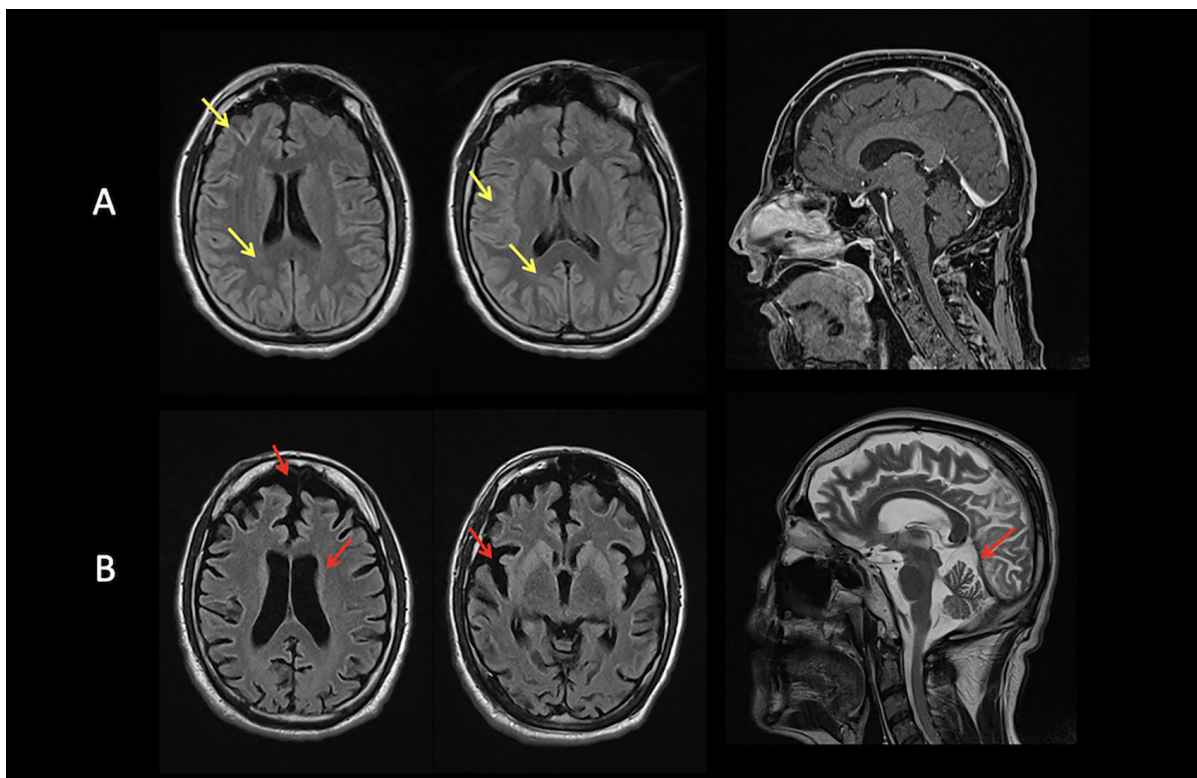


Figure 4 MRI studies from Patient 1. (A) At age 37 years: T₂-FLAIR subcortical hyperintense non-enhancing foci localized to the frontal, temporo-occipital and visual cortices bilaterally with prominent involvement of calcarine cortex (yellow arrows). (B) At age 38 years: severe and diffuse cortical and subcortical atrophy (red arrows).

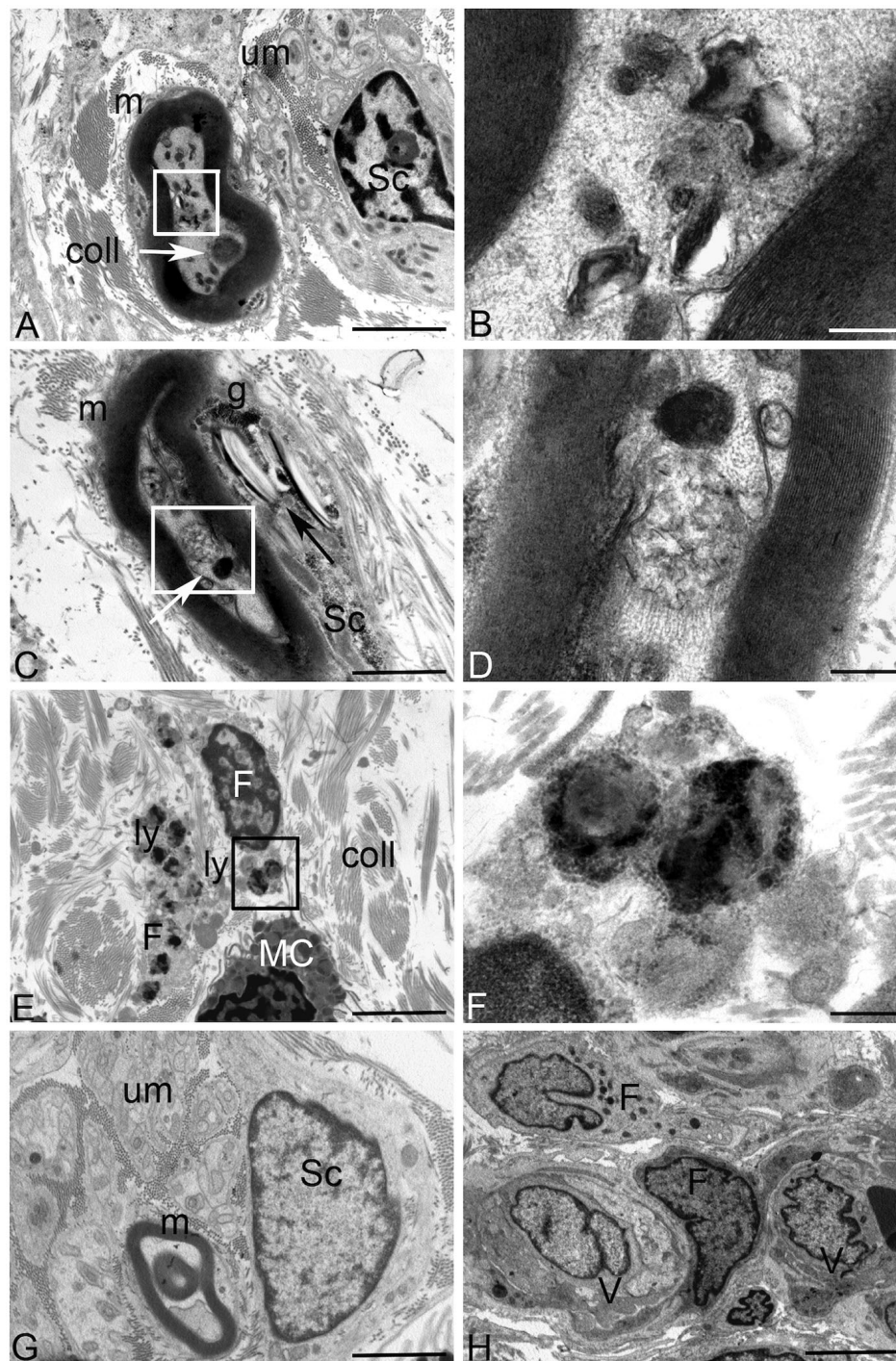


Figure 5 Ultrastructural analysis of the skin biopsy from DHDDS Patient 1 (A–D) compared to control (G and H). (A) No ultrastructural alterations are visible in the unmyelinated nerve fibres in the stroma (um). Deposits of osmyophilic materials are observed in myelinated (m) nerve fibres (white arrow) along with numerous vacuoles containing lamellated membrane structures resembling phospholipids (white square). Stromal collagens (coll) structure was conventional. Sc = Schwann cell. (B) Higher magnification of the area included in the white square of A: Single membrane-surrounded vacuoles containing lamellated membrane structures resembling phospholipids are visible in the axon of myelinated fibres. (C) Deposits of osmyophilic materials are observed in myelinated (m) nerve fibres (white arrow) along with vacuoles containing membranous structures of probable lipid origin. Cholesterol/lipid-like deposits (black arrow) associated with glycogen (g) are visible in the cytoplasm of Schwann cells (Sc). (D) Higher magnification of the area included in the white square of B: deposits of osmyophilic materials and a single-membrane-surrounded vacuole containing membranous structures of probable lipid origin are visible. (E) Stromal fibroblasts (F) containing large secondary lysosomes (ly) are visible in the stroma. coll = collagen; MC = mast cell. (F) Higher magnification of the area included in the black square of E. Large secondary lysosomes filled with different electron-density substances are visible in the cytoplasm of stromal fibroblasts. (G) No ultrastructural alterations are visible in the unmyelinated (um), myelinated (m) nerve fibres or Schwann cells (Sc) in a not pathological skin biopsy. (H) No ultrastructural alterations are visible in the stromal fibroblasts (F) or in vessels (V) in a not pathological skin biopsy. Scale bars = 2 μm (A, C, E, G and H) and 200 nm (B, D and F).

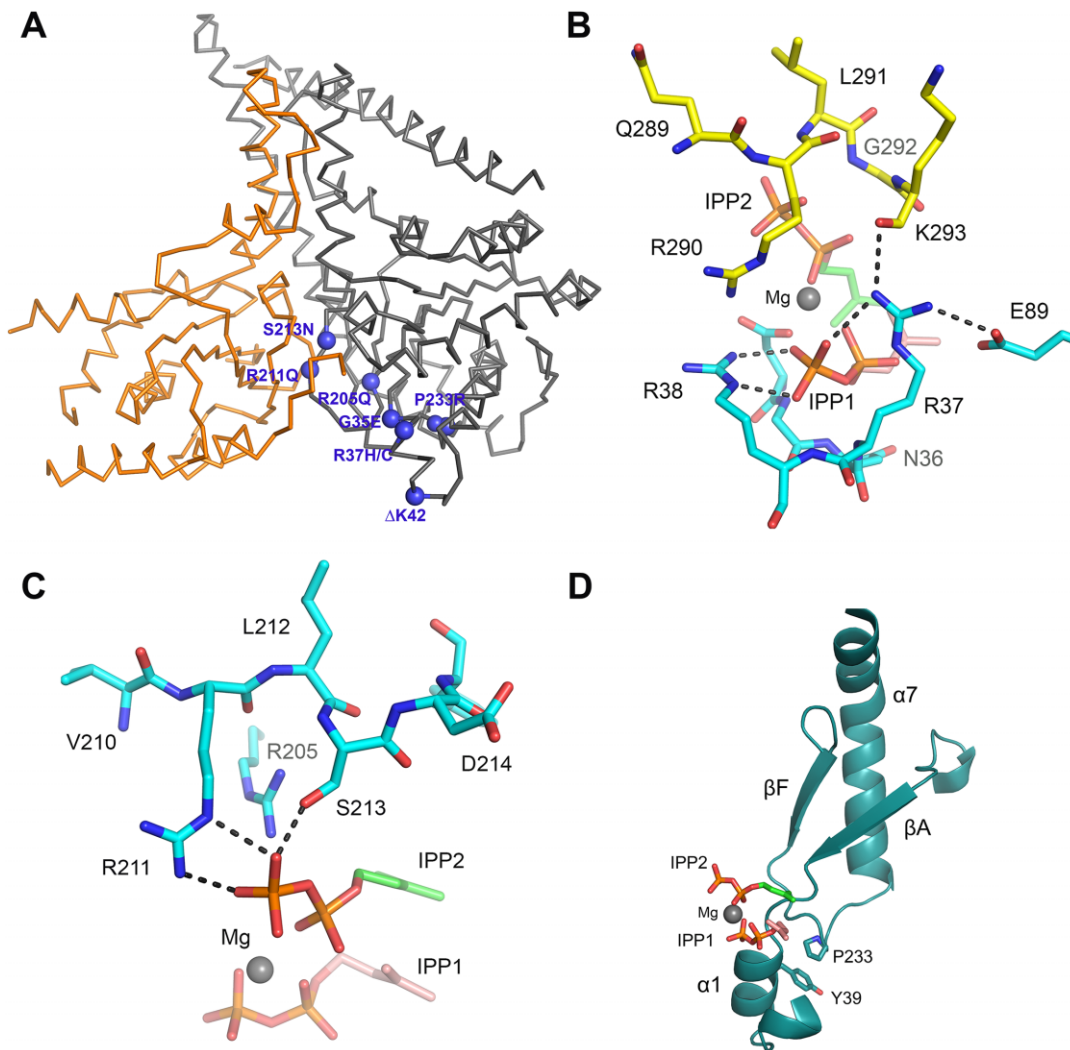


Figure 6 Mapping of *de novo* disease-causing DHDDS variants. (A) Ribbon diagram showing the structure of the NgBR/DHDDS complex (adopted from PDB structure 6W2L). DHDDS mutations are indicated as purple spheres on the structure. NgBR is coloured in orange and DHDDS in grey. Most of the mutations cluster around the active site of the complex, including S213N, R211Q, R205Q, G35E, P233R and R37H/C. An exception is I135T, which is distal to the active site. (B) The side chain of R37 is involved in a network of interactions with the pyrophosphate moiety of the allylic substrate, the side chain of a conserved E89 on DHDDS, and the main chain amide of K293 from the NgBR C-terminal region. Hydrogen bonds are shown as black-dashed lines. Nitrogen atoms are in blue, phosphorus atoms are in orange and oxygen atoms are in red. The carbon atoms of the allylic substrate are shown in salmon and those for the homoallylic substrate are shown in green. Mg²⁺ is shown as a grey sphere. (C) Side chains of R205, R211 and S213 are depicted at the S2 site, and are involved in salt bridging and hydrogen bonding with the pyrophosphate group of the IPP substrate. Replacement of Arg residues with Gln will eliminate these salt bridges and thus weaken IPP binding. Substituting Ser with Asn might result in steric clashes with nearby residues, thereby destabilizing the structure. (D) Ribbon diagram showing the side chain of P233 involved in hydrophobic packing against Y39, which is located at the α1 helix known to harbour important residues for FPP binding. A P233R mutation will disrupt this packing interaction and may destabilize the α1 helix.

information by Hamdan et al.²¹). Newly identified variants were distributed as follows: four patients carried the p.Arg37Cys substitution, two patients carried the p.Gly35Glu, while p.Pro233Arg, p.Ser213Asn, p.Arg205Gln and p.Lys42del were identified in single individuals.

None of these variants was predictive of disease severity in terms of cognitive functioning, epilepsy and movement disorder phenotype. Moreover, the phenotype associated with the three most frequent variants detected in this cohort, namely p.Arg37His, p.Arg37Cys and p.Arg211Gln, did not differ significantly in terms of age of disease onset, clinical presentation pattern or disease course. No specific variants were associated with a better cognitive outcome (Patients 3, 12, 17, 19, 20, 23), while disease course in patients less cognitively compromised (Patients 12, 17, 23) seemed

to be characterized by a later onset and milder epilepsy and movement disorder, regardless of the specific variant. Indeed, the p.Arg37His and p.Arg211Gln were found to occur with a substantially variable clinical phenotype.

Some genotype–phenotype correlations, however, emerged in our cohort. Patients harbouring the p.Arg37His change all suffered from febrile seizures as a presenting feature or during the disease course and epilepsy remained well controlled in three-quarters of patients. The p.Arg211Gln variant was also associated with a severe phenotype, with stepwise deterioration in 2 of 11 patients and fluctuations or exacerbations of movement disorder in 3 of 11 patients. Movement disorders in this subgroup tended to become particularly severe over the disease course. Four of eight patients of this cohort who developed parkinsonism harboured the

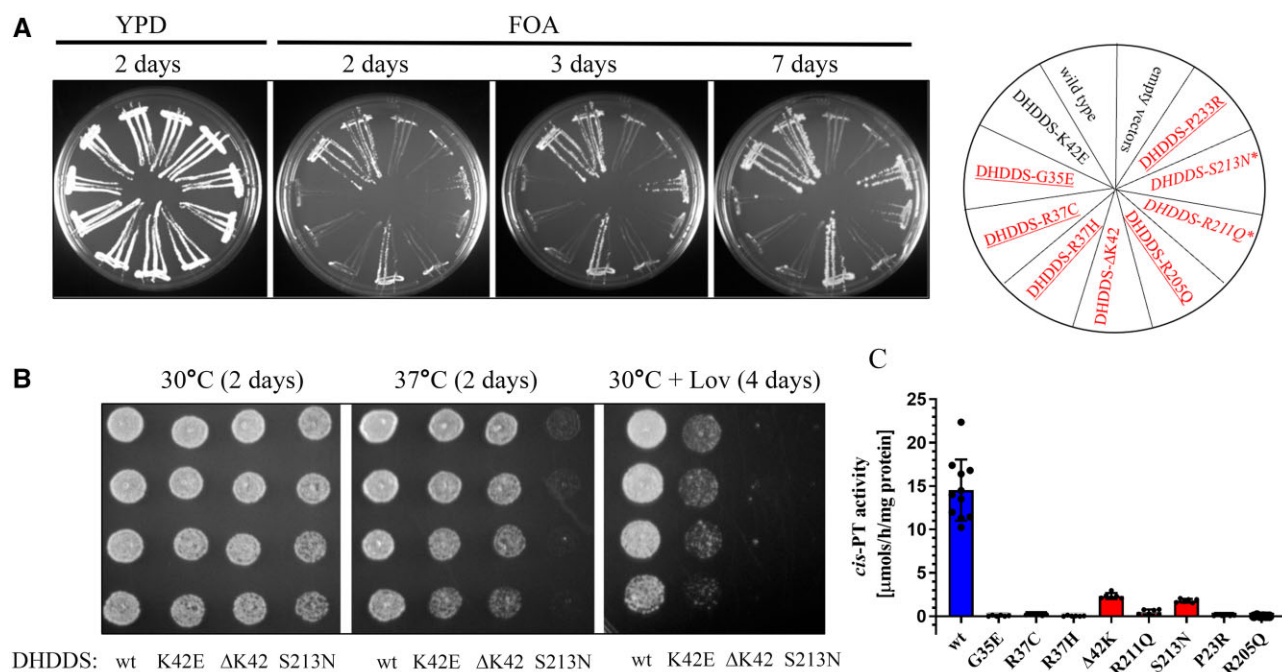


Figure 7 Functional analysis of DHDDS mutants in yeast *Saccharomyces cerevisiae* complementation system and measurement of hcisPTase activity. (A) The *rer2Δ*, *srt1Δ*, *nus1Δ* triple deletion strain expressing *G. lamblia* cis-PT from URA3 plasmid was co-transformed with the *LEU2* and *MET15* plasmids overexpressing wild-type or mutated variant of DHDDS with wild-type NgBR. The cells were streaked onto complete plates (YPD) or synthetic complete medium containing 1% fluorouracil (FOA). The Ura3 protein, which is expressed from the URA3 marker present in the plasmid, converts FOA to toxic 5-fluorouracil. The growth of cells was monitored over time to assess phenotypic differences. The combination of alleles affecting growth is marked with asterisks, and the combination of alleles not supporting growth is underlined. Mutated alleles expressed in patients are indicated in red. (B) Yeast cells lacking endogenous yeast cis-PTase subunits but co-expressing human DHDDS under native *RER2* promoter from centromeric plasmid and NgBR were grown overnight in liquid YPD medium. Cells were diluted to a final concentration of 0.8 optical density units per 1 ml in water, and then 3 μl of each suspension and three subsequent 10-fold serial dilutions were each spotted onto YPD or YPD supplemented with 250 μg/ml of lovastatin (Lov). Cells were incubated at 30 and 37°C up to 4 days to assess phenotypic differences. (C) Cis-PTase activity was measured using purified wild-type DHDDS/NgBR complex or heteromeric complex formed with DHDDS disease mutants as described in the 'Materials and methods' section. Each mutation exhibits reduced cis-PTase activity compared to the wild-type enzyme. G35E, R37C, R37H, R205Q and P233R mutations result in a complex with activity at the detection threshold. Values are expressed as mean ± standard deviation of at least six independent measurements.

p.Arg211Gln variant. Among the five patients with severe psychiatric manifestations, three carried the p.Arg211Gln variant (Patients 1, 6 and 17) while two carried the p.Arg37Cys variant (Patients 8 and 13).

Structural data

The recently resolved structure of the human NgBR/DHDDS complex^{2,6} was used to explore the structural and functional consequences of the identified disease-causing variants. The mutated residues are localized within the previously established cis-PTase catalytic domain of DHDDS (residues 25–265). As shown in Fig. 6A, most amino acid changes affect residues that cluster around the active site of DHDDS and are involved in allylic (farnesyl diphosphate, FPP) and homoallylic (IPP) substrate binding. The β-phosphate group of the FPP substrate is hydrogen-bonded to the backbone amide of Gly35, which is localized on the P-loop, and is well established to be involved in FPP binding. Therefore, replacing Gly35 with Glu35 would result in steric clashes with nearby residues and hence perturb packing of the P-loop and potentially disrupt Arg38 conformation on the preceding α1 helix, which is also involved in FPP binding. In addition, the side chain of Arg37 is stabilized by a network of salt bridges with the β-phosphate group of FPP, Glu89 on DHDDS and the main chain carboxylate group of Lys293 on the C-terminus of NgBR (Fig. 6B). Introducing a histidine residue at this position would abolish binding interactions with the β-phosphate group of FPP substrate as well as with the C-terminus of NgBR. The introduction of a cysteine at this position

could be more detrimental due to the loss of a positive charge. Similarly, the side chains of Arg205 and Arg211 form salt bridges with the pyrophosphate of IPP (Fig. 6C), and replacement of either residue with Gln would eliminate binding interactions with IPP. Although substituting Ser213 with Asn can still maintain hydrogen bonding with the β-phosphate group of IPP, introducing a bulky side chain at this region would result in steric clashes with nearby residues, hence leading to structural destabilization. While the aforementioned residues are directly involved in substrate binding, Pro233 is an exception to this pattern. Pro233 is localized within a loop that connects βF with α7 and seems to be involved in hydrophobic packing against Tyr39 on α1, harbouring FPP binding residues (Fig. 6D). Accordingly, substituting Pro with a charged residue like Arg could disrupt packing of the α1 helix and binding to the FPP substrate. Finally, previous structural and functional studies on the p.K42E substitution have already established its indirect role in FPP binding by stabilizing the α1-helix through a salt bridge formed with a conserved E234.² Similarly, a deletion at this position (ΔK42) could affect the stability of the structure as well as FPP substrate binding.

Functional validation of *de novo* DHDDS missense variants

Yeast complementation assays were performed to functionally validate the identified variants.⁴ As seen in Fig. 7A, mutants containing DHDDS^{ΔK42} were able to support the growth of *rer2Δ/srt1Δ/nus1Δ* yeast cells (lacking endogenous genes critical for cis-PTase

activity) in a manner similar to that of wild-type cis-PT and DHDDS^{K42E} (a mutation underlying retinitis pigmentosa).⁵ DHDDS^{S213N} causes slight growth defect suggesting that enzyme activity is below 20% and that DHDDS^{R211Q} severely impairs yeast growth. Finally, DHDDS^{G35E}, DHDDS^{R37C}, DHDDS^{R37H}, DHDDS^{R205Q} and DHDDS^{P233R} did not support yeast growth, further confirming their predicted essential role in enzymatic activity. To expand the detection limit of our yeast complementation assay, we modified our system by expressing DHDDS from a single-copy plasmid under the native yeast RER2 promoter. Since NgBR is stable in yeast cells only when co-expressed with DHDDS and its co-expression from the single plasmid does not support the growth (data not shown), we generated yeast strains of interest co-expressing DHDDS from a single-copy plasmid and NgBR from a multi-copy plasmid.

We compared the growth rates of yeast expressing either wild-type or one of the DHDDS mutants using the yeast spot test (Fig. 7B) and kinetic growth assay (Supplementary Fig. 1) on yeast extract peptone dextrose (YPD) medium or YPD supplemented with lovastatin, an inhibitor of HMG-CoA reductase, the rate-limiting enzyme of the mevalonate pathway responsible for substrate synthesis. The results showed that yeast cells harbouring the mutated version of DHDDS displayed different degrees of growth delay in YPD medium, with a more pronounced phenotype at 37°C. As expected, these cells were also more sensitive to lovastatin due to the low substrate levels.

Next, we compared the steady-state activities of purified mutants to those of the wild-type complex. As shown in Fig. 4C, all mutants analysed displayed lower enzymatic activity compared to the wild-type enzyme. In addition, mutations that did not support yeast growth (DHDDS^{G35E}, DHDDS^{R37C}, DHDDS^{R37H}, DHDDS^{R205Q} and DHDDS^{P233R}) were able to incorporate radioactive IPP substrate within the detection limit range, suggesting that they formed a catalytically dead enzyme. Overall, enzymatic activity changes were proportional to the level of growth defect observed in our yeast studies. In summary, the data presented herein further support the pathogenicity of the identified *de novo* DHDDS variants.

Discussion

DHDDS phenotypic spectrum

Here, we report a first comprehensive description of the phenotype associated with *de novo* DHDDS variants. We demonstrated that heterozygous DHDDS mutations are associated with a complex slowly progressive CNS disorder with broad functional consequences including cognitive impairment, abnormal motor control (myoclonus, cortical tremor, ataxia, movement disorder) and epilepsy.

We depicted a distinctive disorder presenting during infancy or childhood with neurodevelopmental and neurological findings including GDD/ID, epilepsy, myoclonic movements, and postural and intention tremor (with or without ataxia). Starting from the second decade of life, the disease followed a slow or stepwise pattern of progression, at times, punctuated by episodes of acute deterioration. Cortical tremor generalized, and further signs of diffuse neurological impairment appeared, including epilepsy (when not already present), hyperkinetic and hypokinetic movement disorder, cognitive decline and psychiatric disturbances.

The epileptic phenotype was characterized by febrile seizures at presentation, coexistence of multiple generalized seizure types and an EEG pattern of ictal and interictal generalized slow spike-wave complexes, as also described in two previously reported patients with dominant mutations in DHDDS^{22,23} and in a patient with heterozygous NUS1 pathogenic variants.²⁵

Neuroimaging studies do not contribute to diagnosis or clinical monitoring. No metabolic biomarkers have been associated with the disease. The electrophysiological investigations of the abnormal movements are in support of an exaggerated cortical hyperexcitability state as reported in other myoclonic syndromes.^{23,40,41}

Consistent with this hypothesis, short latency somatosensory evoked potentials (SEPs) showed exaggerated cortical responses (giant SEPs) in a previously reported 15-year-old female with the most recurrent p.Arg211Gln variant and cortical myoclonic tremor,²³ and back-averaged EEG indicated a cortical origin of tremor in three patients of this cohort thus suggesting cortical tremor.

Functional impact of DHDDS pathogenic variants

We provided a first genotype–phenotype correlation analysis supported by functional studies using yeast complementation assay and *in vitro* activity measurements.

Mapping the disease-causing *de novo* DHDDS variants into the protein structure revealed that most cluster around the active site of the DHDDS subunit and probably directly affect enzymatic activity and/or substrate binding. Our findings indicated that all the identified variants formed cis-PTase with impaired/reduced enzymatic activity and show growth defects in yeast complementation assays. DHDDS^{AK42} and DHDDS^{S213N} had a less severe phenotype compared to the other mutants. The impact of these changes on yeast growth became evident only in spot test (37°C) and kinetic growth assay performed in the presence of lovastatin, but was significantly higher compared to that of the recessive retinitis pigmentosa-causing DHDDS^{K42E} mutant.

Molecular mechanisms of DHDDS-related diseases

DHDDS encodes a protein involved in dolichol biosynthesis on the cytoplasmic face of the ER, where N-glycosylation, O-mannosylation, C-mannosylation and GPI-anchor synthesis occurs. Besides the presence of glycosylated dolichol species in the ER, dolichol is present in all subcellular membrane systems. Free alcohol and phosphorylated and esterified dolichol, are detected in peroxisomes and are highly enriched in lysosomes, the plasma membrane and Golgi vesicles.³⁴

Mitochondrial membranes and nuclei also contain a limited amount of dolichol. Furthermore, dolichol plays a more general role in membrane trafficking, particularly between the ER and the lysosomal–endosomal system.³⁵ Given the ubiquity of dolichol in different cellular compartments, dolichol biosynthesis defects and accumulated dolichol precursors can presumably affect many other cellular processes independent of protein post-translational modifications. Interestingly, dolichol accumulation has been reported in neuronal ceroid lipofuscinosis (NCLs),^{36–38} in which retinal degeneration occurs, while alterations in dolichol/Dol-P levels have been reported in patients with Alzheimer's disease.³⁹

Understanding the molecular mechanisms of DHDDS-related diseases is not trivial. Before the recent description of autosomal dominant forms,^{21–23} recessive inheritance was described in a fatal case with severe multi-organ involvement¹⁵ as well as in isolated retinitis pigmentosa.^{16–18} Assuming that human cis-PTase forms a heterodimer under physiological conditions, variants with a loss-of-function/hypomorphic behaviour may lead to dolichol levels that are below the threshold necessary to fulfil its various biological roles in cells. The dolichol threshold concept could explain why heterozygous parents and siblings of patients carrying the p.Lys42Glu substitution underlying retinitis pigmentosa or the p.Trp64/p.Cys148Glu changes (DHDDS) and p.Arg290His (NgBR)⁴ associated with CDG type I appear to be healthy individuals.^{15–18}

Indeed, the probability of being loss-of-function intolerant (pLI score, gnomAD v.2.1.1), a metric used to determine the tolerance of a gene for loss-of-function variants, supports DHDDS is not haploinsufficient (pLI = 0.25).

Interestingly, a recent study on the human NgBR/DHDDS complex suggested a higher oligomerization state of the complex whereby the two heterodimers were depicted to form a tetramer.⁶ This observation introduces the possibility of a dominant-negative mechanism that may reduce cis-PTase activity of certain mutants to lower levels than expected. Based on these findings, we suggest the homozygosity for loss-of-function or strong hypomorphic variants underlies CDG type I (both DHDDS and NgBR), while *de novo* pathogenic variants are likely to have a dominant-negative effect on heterodimer/tetramer assembly and function.

On the other hand, it has been suggested that p.Lys42Glu may affect only retinal photoreceptors because the highest level of DHDDS/NgBR enzymatic activity is required in this tissue for opsin N-glycosylation.¹⁶ Consistent with zebrafish studies indicating that a slight downmodulation of the endogenous gene is sufficient to cause photoreceptor degeneration, whereas a stronger knock-down causes a more complex phenotype, this change might be tolerated outside the retina.¹⁷ This model, however, does not explain why the retina is not affected in individuals carrying dominant DHDDS pathogenic variants, suggesting a more complex scenario for these substitutions. In line of principle, single nucleotide changes at codon 42, not encompassing a CpG site, are predicted to lead to multiple amino acid substitutions, i.e. Gln and Glu (first position), Thr, Arg and Met (second position), and Asn (third position). The invariant association of retinitis pigmentosa with p.Lys42Glu suggests a neomorphic effect for this change or, more likely, a deleterious effect restricted to the retina (e.g. altered interaction of defective DHDDS with a photoreceptor-specific protein or a tissue-specific toxic effect of accumulating isoprenoid compounds).^{16,19} In line with this hypothesis, in patients with DHDDS-related retinitis pigmentosa as well as in other CDGs involving dolichol metabolism,³² D18 becomes the dominant species, with altered plasma and urinary D18/D19 ratios and a possible accumulation of damaging precursors in the retina.²⁰ Of note, the urinary dolichol D18/D19 ratio determined by LC-MS/MS was normal in patients carrying *de novo* DHDDS variants.

Finally, it is also worth noting that the broad phenotypic spectrum amongst patients harbouring the common p.Arg211Gln mutation suggests additional factors, including environmental and genetic background, which may contribute to the final clinical picture.

Aberrant NgBR/DHDDS complex functioning is associated with a neurodegeneration and myoclonus

The association between generalized epilepsy and cortical tremor or other myoclonic phenomena, which patients with Alzheimer's disease pathogenic DHDDS and NUS1 variants share, places the two disorders in the differential diagnosis of several syndromes in the cortical myoclonus spectrum, including progressive myoclonus epilepsy-ataxia (PME/PMA), and, for patients with milder presentations, benign adult familial myoclonus epilepsy.^{22,25,41}

Furthermore, the relatively high movement disorder incidence, including parkinsonism in patients with *de novo* DHDDS and NUS1 pathogenic variants, is indicative of a possible contribution of the NgBR-DHDDS complex to the pathogenesis of Parkinson's disease and neurodegenerative processes. In line with this finding Guo *et al.*²⁶ reported that NUS1 loss could reduce the number of dopaminergic neurons with apoptosis in the fly brain.

Overall, the prominent neurological phenotype of our cohort highlights the importance of dolichol metabolism in neuronal sub-cellular membrane systems and further broaden the clinical and biochemical characterization of DHDDS-related conditions, placing them in a spectrum that only partially overlaps with CDG type I. In line with this, serum glycoprotein hypoglycosylation was not observed in these patients and, in contrast to the retinitis pigmentosa phenotype²⁰ and other CDGs involving dolichol metabolism,^{4,32} the urinary dolichol D18/D19 ratio determined by LC-MS/MS was normal. Instead, electron microscopy of skin biopsy revealed abundant lipid-like material storage in myelinated fibres and Schwann cells, and secondary lysosomes in stromal fibroblasts suggesting a dysfunction of lysosomal enzymatic digestion machinery.

Consistently with this finding lysosomal cholesterol accumulation has been recently reported in fibroblasts of patients with *de novo* NUS1 and DHDDS pathogenic variants.^{42,43} Given that many lysosomal enzymes are highly N-glycosylated, hypo-glycosylation caused by impaired dolichol synthesis may be contributing factor to the neurological symptoms observed in the patients with defective DHDDS or NUS1.⁴³

The aberrant functioning of the ER-endolysosomal pathway and the association between cortical myoclonus, severe movement disorder including parkinsonism, neurological deterioration, cerebral atrophy and storage material in myelinated fibres and fibroblasts, supports the proximity of DHDDS-related disorders to other inherited storage diseases such as NCLs and other lysosomal disorders.

Additional functional studies with future generation of knock-out/knock-in mice and induced pluripotent stem cell-derived neuronal cell models could provide a full understanding of the consequences of these and other DHDDS mutations on cellular organelle dynamics, dolichol metabolism, mammalian brain development and neurodegeneration pathways. Many aspects of dolichol-dependent glycosylation including N-glycosylation, several steps of synthesis, recycling and regulation of dolichol availability are still largely unknown. This information would be critical not only to understand the biochemical underpinning of this disease, but also to consider the potential for specific disease-targeted therapeutic interventions.

Funding

Z.G.O. is supported by the Fonds de recherche du Québec-Santé Chercheur-Boursier award and is a Parkinson Canada New Investigator awardee. EUROGLYCAN-omics (H.H., L.Z.) was supported by Ministry of Education Youth and Sports of Czech Republic No. 8F19002, and (D.J.L.) by the Netherlands Organisation for Health Research and Development (90030376501) under the frame of E-Rare-3, the ERA-Net for Research on Rare Diseases. This work was also supported by NIH Grant R35 HL139945 and RO1 DK125492 (to W.C.S.) and the NIH's Common Fund, Office of the Director of the NIH to the NIH Undiagnosed Diseases Program (to E.M. and C.T.). A.B. and I.B. received funding specifically appointed to Department of Medical Sciences from the Italian Ministry for Education, University and Research (Ministero dell'Istruzione, dell'Università e della Ricerca—MIUR) under the programme 'Dipartimenti di Eccellenza 2018–2022' Project code D15D18000410001. M.T. is supported by the Italian Ministry of Health (Ricerca Corrente).

Competing interests

Z.G.O. received consultancy fees from Lysosomal Therapeutics Inc. (LTI), Idorsia, Preval Therapeutics, Inceptions Sciences (now

Ventus), Ono Therapeutics, Neuron23, Handl Therapeutics, Denali, Bial, Lighthouse, Guidepoint and Deerfield. D.S. consulted for Upsher-Smith, Biomarin, Neurogene Marinus and Ovid Therapeutics on unrelated subject matter. He also serves on the advisory board for the non-profit foundations SLC6A1 Connect and FamilieSCN2A.

Supplementary material

Supplementary material is available at Brain online.

References

- Grabińska KA, Park EJ, Sessa WC. cis-Prenyltransferase: New insights into protein glycosylation, rubber synthesis, and human diseases. *J Biol Chem*. 2016;291(35):18582–18590.
- Edani BH, Grabińska KA, Zhang R, et al. Structural elucidation of the cis-prenyltransferase NgBR/DHDDS complex reveals insights in regulation of protein glycosylation. *Proc Natl Acad Sci U S A*. 2020;117(34):20794–20802.
- Harrison KD, Park EJ, Gao N, et al. Nogo-B receptor is necessary for cellular dolichol biosynthesis and protein N-glycosylation. *EMBO J*. 2011;30(12):2490–2500.
- Park EJ, Grabińska KA, Guan Z, et al. Mutation of Nogo-B receptor, a subunit of cis-prenyltransferase, causes a congenital disorder of glycosylation. *Cell Metab*. 2014;20(3):448–457.
- Grabińska KA, Edani BH, Park EJ, Kraehling JR, Sessa WC. A conserved C-terminal RXG motif in the NgBR subunit of cis-prenyltransferase is critical for prenyltransferase activity. *J Biol Chem*. 2017;292(42):17351–17361.
- Bar-El ML, Vaňková P, Yeheskel A, et al. Structural basis of heterotetrameric assembly and disease mutations in the human cis-prenyltransferase complex. *Nat Commun*. 2020;11(1):5273.
- Chojnacki T, Dallner G. The biological role of dolichol. *Biochem J*. 1988;251(1):1–9.
- Freeze HH. Genetic defects in the human glycome. *Nat Rev Genet*. 2006;7(7):537–551.
- Jaeken J, Matthijs G. Congenital disorders of glycosylation: A rapidly expanding disease family. *Annu. Rev. Genomics Hum. Genet*. 2007;8:261–278.
- Cantagrel V, Lefeber DJ. From glycosylation disorders to dolichol biosynthesis defects: A new class of metabolic diseases. *J Inherit Metab Dis*. 2011;34(4):859–867.
- Buczowska A, Swiezewska E, Lefeber DJ. Genetic defects in dolichol metabolism. *J Inherit Metab Dis*. 2015;38(1):157–169.
- Cantagrel V, Lefeber DJ, Ng BG, et al. SRD5A3 is required for converting polyprenol to dolichol and is mutated in a congenital glycosylation disorder. *Cell*. 2010;142(2):203–217.
- Cherepanova N, Shrimal S, Gilmore R. N-linked glycosylation and homeostasis of the endoplasmic reticulum. *Curr Opin Cell Biol*. 2016;41:57–65.
- De Giorgi M, Jarrett KE, Burton JC, et al. Depletion of essential isoprenoids and ER stress induction following acute liver-specific deletion of HMG-CoA reductase. *J Lipid Res*. 2020;61(12):1675–1686.
- Sabry S, Vuillaumier-Barrot S, Mintet E, et al. A case of fatal Type I congenital disorders of glycosylation (CDG I) associated with low dehydrodolichol diphosphate synthase (DHDDS) activity. *Orphanet J Rare Dis*. 2016;11(1):84.
- Zelinger L, Banin E, Obolensky A, et al. A missense mutation in DHDDS, encoding dehydrodolichyl diphosphate synthase, is associated with autosomal-recessive retinitis pigmentosa in Ashkenazi Jews. *Am J Hum Genet*. 2011;88(2):207–215.
- Züchner S, Dallman J, Wen R, et al. Whole-exome sequencing links a variant in DHDDS to retinitis pigmentosa. *Am J Hum Genet*. 2011;88(2):201–206.
- Lam BL, Züchner SL, Dallman J, et al. Mutation K42E in dehydrodolichol diphosphate synthase (DHDDS) causes recessive retinitis pigmentosa. *Adv Exp Med Biol*. 2014;801:165–170.
- Fliesler SJ, Tabor GA, Hollyfield JG. Glycoprotein synthesis in the human retina: Localization of the lipid intermediate pathway. *Exp Eye Res*. 1984;39(2):153–173.
- Wen R, Lam BL, Guan Z. Aberrant dolichol chain lengths as biomarkers for retinitis pigmentosa caused by impaired dolichol biosynthesis. *J Lipid Res*. 2013;54(12):3516–3522.
- Hamdan F, Myers C, Cossette P, et al.; Deciphering Developmental Disorders Study. High rate of recurrent *de novo* mutations in developmental and epileptic encephalopathies. *Am J Hum Genet*. 2017;101(5):664–685.
- Togashi N, Fujita A, Shibuya M, et al. Fifteen-year follow-up of a patient with a DHDDS variant with non-progressive early onset myoclonic tremor and rare generalized epilepsy. *Brain Dev*. 2020;42(9):696–699.
- Piccolo G, Amadori E, Vari MS, et al. Complex neurological phenotype associated with a De Novo DHDDS mutation in a boy with intellectual disability, refractory epilepsy, and movement disorder. *J Pediatr Genet*. 2021;10(3):236–238.
- Den K, Kudo Y, Kato M, et al. Recurrent NUS1 canonical splice donor site mutation in two unrelated individuals with epilepsy, myoclonus, ataxia and scoliosis - a case report. *BMC Neurol*. 2019;19(1):253.
- Araki K, Nakamura R, Ito D, et al. NUS1 mutation in a family with epilepsy, cerebellar ataxia, and tremor. *Epilepsy Res*. 2020;164:106371.
- Guo JF, Zhang L, Li K, et al. Coding mutations in NUS1 contribute to Parkinson's disease. *Proc Natl Acad Sci U S A*. 2018;115(45):11567–11572.
- Philippakis AA, Azzariti DR, Beltran S, et al. The matchmaker exchange: A platform for rare disease gene discovery. *Hum Mutat*. 2015;36(10):915–921.
- Scheffer IE, Berkovic S, Capovilla G, et al. ILAE classification of the epilepsies: Position paper of the ILAE Commission for Classification and Terminology. *Epilepsia*. 2017;58(4):512–521.
- Li Q, Wang K. InterVar: Clinical interpretation of genetic variants by the 2015 ACMG-AMP guidelines. *Am J Hum Genet*. 2017;100(2):267–280.
- Richards S, Aziz N, Bale S, et al.; ACMG Laboratory Quality Assurance Committee. Standards and guidelines for the interpretation of sequence variants: A joint consensus recommendation of the American College of Medical Genetics and Genomics and the Association for Molecular Pathology. *Genet Med*. 2015;17(5):405–424.
- Lacey JM, Bergen HR, Magera MJ, Naylor S, O'Brien JF. Rapid determination of transferrin isoforms by immunoaffinity liquid chromatography and electrospray mass spectrometry. *Clin Chem*. 2001;47(3):513–518.
- Zdrzilova L, Kuchar L, Ondruskova N, Honzik T, Hansikova H. A new role for dolichol isoform profile in the diagnostics of CDG disorders. *Clin Chim Acta*. 2020;507:88–93.
- Garrett TA, Guan Z, Raetz CR. Analysis of ubiquinones, dolichols, and dolichol diphosphate-oligosaccharides by liquid chromatography-electrospray ionization-mass spectrometry. *Methods Enzymol*. 2007;432:117–143.
- Rip JW, Rupar CA, Chaudhary N, Carroll KK. Localization of a dolichyl phosphate phosphatase in plasma membranes of rat liver. *J Biol Chem*. 1981;256(4):1929–1934.
- Ban Duijn G, Valtersson C, Chojnacki T, Verkleij AJ, Dallner G, de Kruijff B. Dolichyl phosphate induces non-bilayer structures,

- vesicle fusion and transbilayer movement of lipids: A model membrane study. *Biochim Biophys Acta*. 1986;861(2):211–223.
36. Kin NMK, Palo J, Haltia M, Wolfe LS. High levels of brain dolichols in neuronal ceroid-lipofuscinosis and senescence. *J Neurochem*. 1983;40(5):1465–1473.
 37. Faust JR, Rodman JS, Daniel PF, Dice JF, Bronson RT. Two related proteolipids and dolichol-linked oligosaccharides accumulate in motor neuron degeneration mice (mnd/mnd), a model for neuronal ceroid lipofuscinosis. *J Biol Chem*. 1994;269(13):10150–10155.
 38. Jolly RD. Comparative biology of the neuronal ceroid-lipofuscinoses (NCL): An overview. *Am J Med Genet*. 1995;57(2):307–311.
 39. Söderberg M, Edlund C, Alafuzoff I, Kristensson K, Dallner G. Lipid composition in different regions of the brain in Alzheimer's disease/senile dementia of Alzheimer's type. *J Neurochem*. 1992;59(5):1646–1653.
 40. van der Veen S, Zutt R, Klein C, et al. Nomenclature of genetically determined myoclonus syndromes: Recommendations of the International Parkinson and Movement Disorder Society Task Force. *Mov Disord*. 2019;34(11):1602–1613.
 41. Latorre A, Rocchi L, Magrinelli F, et al. Unravelling the enigma of cortical tremor and other forms of cortical myoclonus. *Brain*. 2020;143(9):2653–2663.
 42. Yu S-H, Wang T, Wiggins K, et al. Lysosomal cholesterol accumulation contributes to the movement phenotypes associated with NUS1 haploinsufficiency. *Genet Med*. 2021;23(7):1305–1314.
 43. Courage C, Oliver KL, Park EJ, et al. Progressive myoclonus epilepsies—Residual unsolved cases have marked genetic heterogeneity including dolichol-dependent protein glycosylation pathway genes. *Am J Hum Genet*. 2021;108(4):722–738.